# Modeling and Simulation of Electric Vehicle Drive Control System

Mahmoud Ebrahim Khalil
*Military Technical College, Egypt*

*Supervisor:* Mostafa Yacoub, Assistant Professor
*Military Technical College*

*Abstract– A hybrid car is an automobile which uses two sources of energy. Our hybrid car will use the electric energy and solar energy as in our recent years we show how the internal combustion engine emissions affect the environment around us. So all sights are aimed towards electric vehicles, not only for their environmental role but for other advantages as they are more quiet, more efficient and can be controlled easily. For the ease of control, our vehicle has a DC motor so the required speed can be achieved using a simple controller. The controller used is a PID controller, which consists of a proportional gain with constant KP, a differential gain with constant KD and an integral gain with constant KI. MATLAB/SIMULINK platform enables us to make a simulation for our model and to investigate the response of the system.*

## I. INTRODUCTION

Hybrid Electric Vehicles (HEVs) represent a solution to save fuel and reduce $CO_2$ emissions, powered by a rechargeable energy storage device (e.g., battery or super capacitors) or by using solar energy, [1].

Conventional vehicles provide good performance and long range, but they harm the environment by the exhaust gases. Manufacturers are aiming towards electric vehicles, [2]. The range and speed of electric vehicles are limited compared to the conventional vehicles. With the development of electric motor and battery technology, longer ranges became achievable. Therefore, performance of these vehicles can be optimized by selecting the motors and batteries depending on the region and the drive cycle. In this study, the dynamic model of an electric vehicle was created with MATLAB/Simulink, [3].
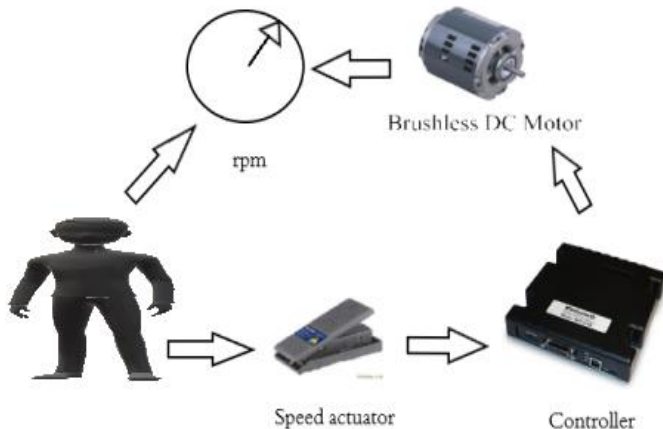


Fig 1. Complete Simulink model of an Electric Vehicle, [2].

The second section of this paper shows mathematical modeling of the DC motor and resistance to vehicle motion. The third section shows the simulation and the results of the developed model. The fourth section illustrates the speed controller design and finally, the fifth section concludes the paper.

## II. MATHEMATICAL Model

### A. Dc Motor

DC motors are characterized by their speed control simplicity while maintaining accurate and smooth speed transitions.

The electric circuit of a DC motor is shown in Fig. 2. The electric equations of the DC motor are as follows, [4]:

$$V_a = i_a R_a + L_a \frac{di_a}{dt} + V_b \qquad (1)$$
$$V_b = K_b \omega \qquad (2)$$

where, $V_a$ is the applied armature voltage, $i_a$ is the armature current, $L_a$ is the armature inductance, $R_a$ is the resistance of the armature, $V_b$ is the back electromagnetic force, $K_b$ is the motor velocity constant and $\omega$ is the motor shaft angular speed. The mechanical equation of the DC motor is:

$$J \frac{d\omega}{dt} = T_m - \sum T_l \qquad (3)$$

where, $J$ is the mass moment of inertia of the motor shaft assembly about its axis of rotation, $T_m$ is the motor driving torque and the last term in (3) is the sum of the resisting (load) torques applied to the motor shaft.
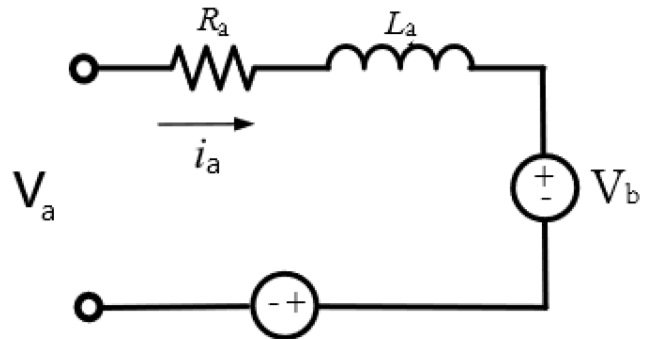
**5th IUGRC International Undergraduate Research Conference,**
**Military Technical College, Cairo, Egypt, Aug 9th – Aug 12st, 2021.**

345

The driving torque of the motor could also be represented by the following equation:

$$T_m = K_m i_a \qquad (4)$$

where, $K_m$ is the motor torque constant. Taking the Laplace transform of (1) to (4) yields

$$T_m = K_m I_a(s) \qquad (5)$$

$$V_a(s) = (R_a + sL_a)I_a(s) + V_b(s) \qquad (6)$$

or,

$$V_a(s) = (R_a + sL_a)I_a(s) + K_b \Omega(s) \qquad (7)$$

$$I_a(s) = \frac{V_a(s) - K_b \Omega(s)}{(R_a + sL_a)} \qquad (8)$$

Then,

$$T_m(s) = \frac{K_m(V_a(s) - K_b \Omega(s))}{R_a + sL_a} \qquad (9)$$

The disturbance torque could be added to the load torque as follows:

$$T_m(s) = T_l(s) + T_d(s) \qquad (10)$$

where, $T_d(s)$ is the Laplace transform of the disturbance torque.

### B. Resistances to Vehicle Motion

During driving, resistance forces act on the vehicles. Fig .3 shows the vehicle resistance forces acting on the longitudinal direction. These resistance forces are;
- Aerodynamic Resistance, $F_{aerodynamic}$
- Tire Rolling Resistance, $F_{roll}$
- Gradient Resistance, $F_{grade}$
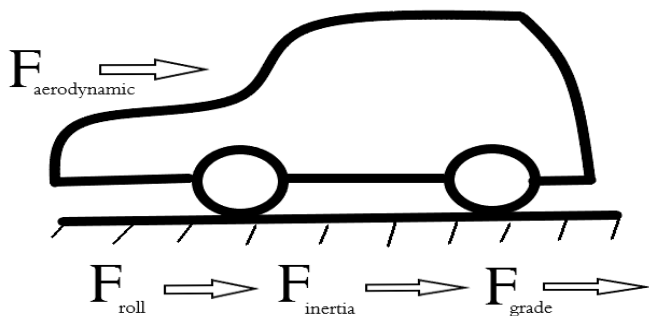- Inertia Resistance, $F_{inertia}$

### 1) Aerodynamic Resistance

Resistance force results from the air drag depends on the shape of the vehicle body and the vehicle speed.

$$F_{aerodynamic} = KFV^2 \qquad (11)$$

where, $K$ is the air drag factor, $F$ is the vehicle projected frontal area and $V$ is the vehicle forward speed. The air drag factor is determined experimentally according to vehicle shape. Table I shows some typical values for frontal areas and air drag factors according for different vehicle types.

TABLE I
AVERAGE VALUES OF FRONTAL AREA F AND THE AIR DRAG FACTOR K

| Vehicle Type | $F(m^2)$ | $K(N.s^2/m^4)$ |
|---|---|---|
| Racing car | 0.4:0.6 | 0.15:0.2 |
| Small passenger car | 1.4:2 | 0.2:.35 |
| Medium high class | 2:2.8 | 0.4:0.5 |
| Lorries | 3:7 | 0.5:0.7 |

### 2) Tire Rolling Resistance

Due to the elastic structure of the wheel, in front of the wheel contact centre, a resistance force against the rotational movement of the tire occurs. The tire rolling resistance is calculated using the following equation:

$$F_{roll} = Gf \cos \alpha \qquad (12)$$

where, $G$ is the gross vehicle weight, $\alpha$ is the gradient (slope) of the path and $f$ is the tire rolling resistance coefficient. The later varies according to the road surface. Table II shows some typical values of rolling resistance coefficients for different types of roads.

TABLE II
TYPICAL ROLLING RESISTANCE COEFFICIENTS FOR DIFFERENT TYPES OF ROADS

| Road Surface | f |
|---|---|
| Concrete or Asphalt | 0.013 |
| Small Gravel Ground | 0.02 |
| Macadamized Road | 0.025 |
| Soil Road | 0.1-0.35 |

### 3) Gradient Resistance

The gradient resistance arises when the vehicle is moving on a ramp road. The gradient resistance appears due to the component of gravity. It is expressed as follows:

$$F_{grade} = G \sin \alpha \tag{13}$$

*4) Inertia Resistance*

The inertia resistance force is calculated using the following equation

$$F_{inertia} = m\theta \frac{dV}{dt} \tag{14}$$

where, $m$ is the gross vehicle mass and $\theta$ is the coefficient of rotating parts. Therefore, total tractive effort $F_{total}$, which is the force required to drive the vehicle, is given by

$$F_{total} = F_{aero} + F_{roll} + F_{grade} + F_{inertia} \tag{15}$$

or,

$$F_{total} = KFV^2 + Gf \cos \alpha + G \sin \alpha + m\,\theta\,\frac{dv}{dt} \tag{16}$$

The load torque applied to the wheel is calculated by ,

$$T_w = F_{total}r \tag{17}$$

where, $r$ is the tire dynamic radius.

The resisting torque applied to the motor shaft, Tl is the transformation of the wheel torque to the motor shaft through the final drive. Then, the motor load torque becomes

$$T_l = (F_{total}r)/K_d \tag{18}$$

where, $K_d$ is the final drive gear ratio.

All the values of the vehicle and DC motor parameters are listed in Table III.

TABLE III
VEHICLE AND DC MOTOR PARAMETERS THAT ARE USED IN THE PRESENTED MODEL.

| Parameter | Value | Unit |
|---|---|---|
| Air drag factor (K) | 0.35 | $Ns^2/m^4$ |
| Vehicle frontal projected area (F) | 2 | $m^2$ |
| Motor armature resistance ($R_a$) | 40 | ohm |
| Inductance of armature ($l_a$) | 5.02 | mH |
| Inertia of motor shaft assembly (J) | 23.3 | $gcm^2$ |
| dynamic radius (r) | 0.25 | m |
| Gross vehicle mass (M) | 550 | kg |
| Coefficient of rotating parts ($\theta$) | 1.1 | - |
| Final drive gear ratio($K_d$) | 12 | - |
| Motor velocity constant ($K_b$) | 173 | rpm/v |
| Motor torque constant ($K_m$) | 55.2 | mNm/A |

**5th IUGRC International Undergraduate Research Conference,**
**Military Technical College, Cairo, Egypt, Aug 9th – Aug 12st, 2021.**

347

To linearize (16) to (18), Taylor series is used. Hence, the quadratic term in (16) becomes

$$V^2 = V_o{}^2 + 2V_o(V - V_o) \tag{19}$$

Choosing the operating point $V_o = 3$ m/s and applying Laplace transform to (18) yields

$$T_l(s) = \frac{\left(KFr\left(V_o{}^2 + 2V_o(V-V_o)\right) + Gfr \cos \alpha + Gr \sin \alpha + m\theta\frac{dV}{dt}\right)}{K_d} \tag{20}$$

When the vehicle is moving on level roads,

$$T_l(s) = \frac{\left(KFr\left(V_o{}^2 + 2V_o(V-V_o)\right) + Gfr + m\theta\frac{dV}{dt}\right)}{K_d} \tag{21}$$

Assuming the tires exhibit pure rolling,

$$T_l(s) = \frac{\left(2KFr^2 V_o\Omega(s) + m\theta rs\Omega(s) - KFrV_o{}^2 + Gfr\right)}{K_d s} \tag{22}$$

By isolating the constant terms in (22) and assuming they are constant disturbance, then

$$T_d(s) = \left(-KFrV_o{}^2 + Gfr\right)/s \tag{23}$$

Using (9), (10) and (23) yields

$$K_m((V_a\,(s) - K_b\,W(s))/(R_a + sL_a\,)) = \\ \left((2KFr^2 V_o W(s) + m\theta rsW(s))/K_d\ + (Js + b)W(s)\right) \tag{24}$$

Fig.4 shows the block diagram of the electric vehicle drive control system, where $V_d$ is the disturbance vehicle forward speed.
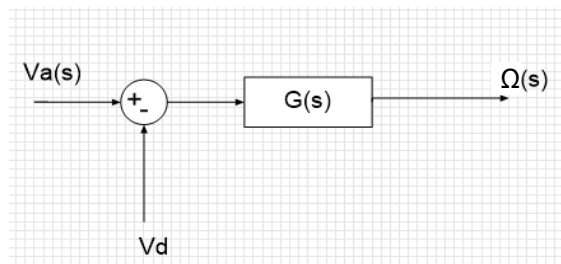


Fig. 4    Block diagram of the electric vehicle drive control system.

III. SIMULATION AND RESULTS

Fig. 5 and Fig.6 show the developed SIMULINK model for the DC motor and the vehicle longitudinal motion, respectively. Fig. 7 shows the load torque applied to the vehicle motor shaft. Fig. 8 and Fig. 9 show the time response of the open-loop system. As shown from figures, the speed response has a high overshoot and a short settling time. This may cause a damage to the vehicle undercarriage during acceleration.
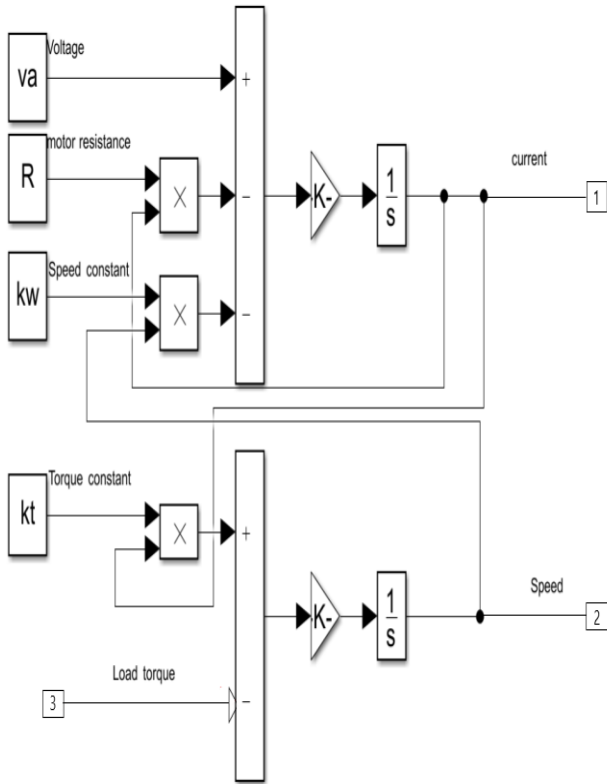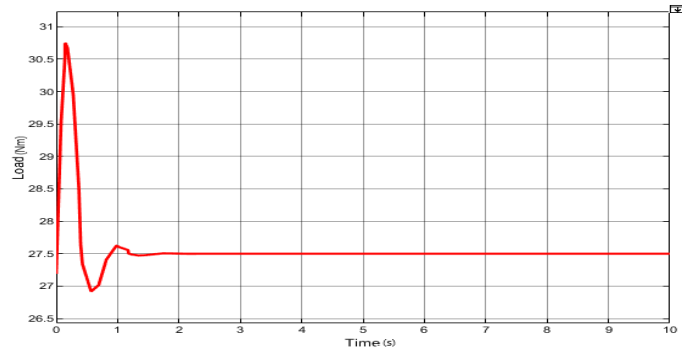
Fig. 5 Motor model using SIMULINK.



Fig.6 Vehicle longitudinal dynamics simulation.



Fig. 7 Load torque applied to the motor shaft.
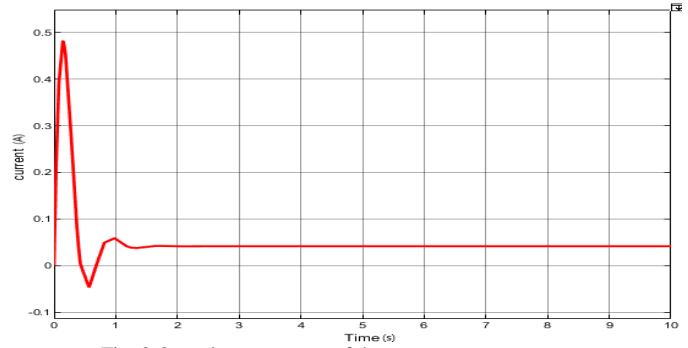


Fig. 8 Open-loop response of the motor armature current.



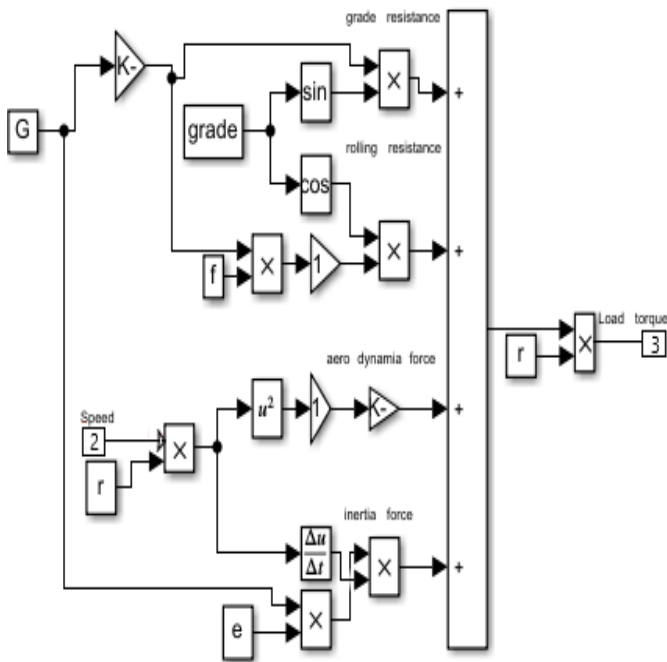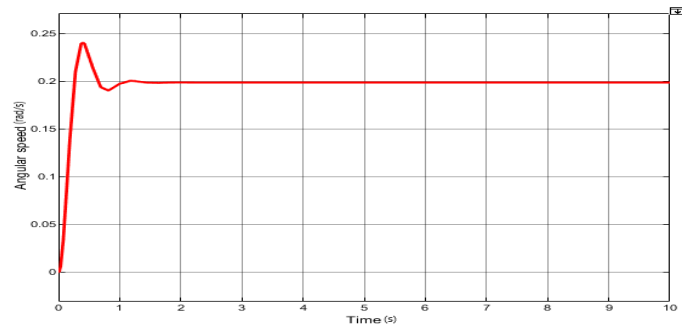Fig. 9 Open-loop time response of the motor angular speed.

Iv. CONTROL SYSTEM DESIGN

Although the main goal of the controller is to regulate the vehicle speed, it is also required to enhance the transient response of the vehicle speed. Achieving a settling time of 2 seconds while maintaining an overshoot of less than 10% is of prime interest in order to achieve a smooth acceleration without causing a damage in the vehicle undercarriage.

The simplest control strategy is to implement a proportional controller to the system. The root locus of the open-loop system represented in (24) is shown in Fig.10. As shown in figure, the system root-locus doesn't pass through the desired pole depicted from the mentioned system requirements. Accordingly, a proportional controller will not achieve the desired system performance. A Proportional-Integral-Derivative (PID) controller was used to achieve that goal.

**5th IUGRC International Undergraduate Research Conference,**
**Military Technical College, Cairo, Egypt, Aug 9th – Aug 12st, 2021.**

348

Fig. 11 shows the developed SIMULINK model for the PID controller. The controller components' gains were calculated using Zeigler-Nichols method. Table IV shows the values of the gains and the achieved response parameters (settling time, rise time and overshoot). Fig. 12 shows the Bode plot of the closed-loop system while Fig. 13 shows the time response of the closed-loop speed control system. As shown in figures, the proposed control system succeeded to achieve the desired response characteristics.
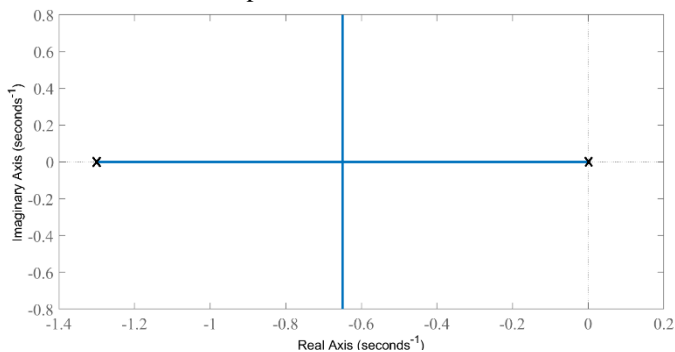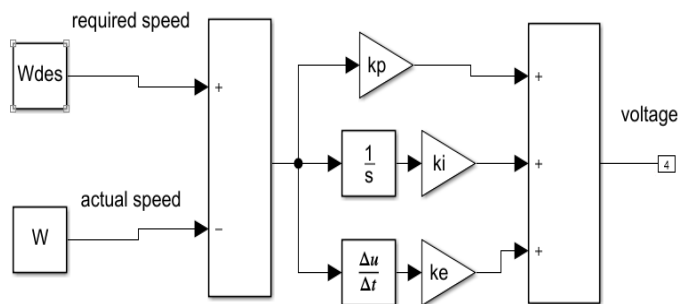

Fig.10 System root locus.


Fig.11 PID simulation using SIMULINK, [3].

TABLE IV
VALUES OF CONTROLLER GAINS AND THE RESPONSE PERFORMANCE PARAMETERS.

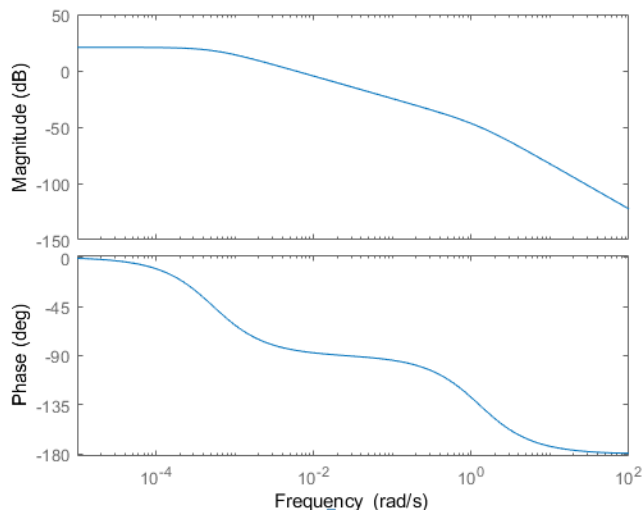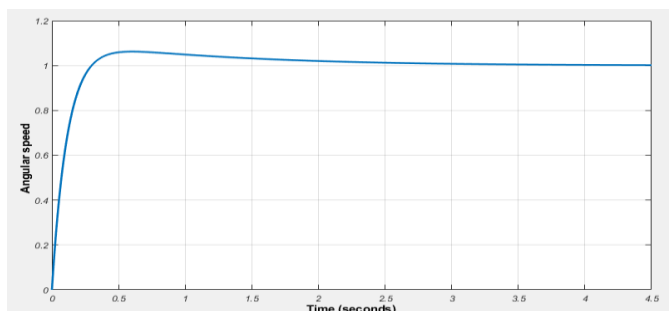| Parameter | Value |
|---|---|
| Proportional gain $K_p$ | 2615.4486 |
| Integral gain $K_i$ | 1346.3289 |
| Derivative gain $K_d$ | 1270.2267 |
| Rise time | 0.193 seconds |
| Settling time | 2 seconds |
| Over shoot | 6.22 % |
| Peak | 1.06 |
| Closed loop Stability | Stable |


Fig.12 Bode diagram


Fig. 13 Closed-loop speed response.

## V. CONCLUSION

A simplified mathematical model for an electric vehicle was proposed. The model considered the electric and mechanical equations of the DC electric motor. The forward dynamics model for the vehicle was carried out. A SIMULINK model for the electric vehicle was developed. The time response of the vehicle was evaluated. In order to enhance the speed response of the vehicle, a PID control system was implemented. The closed-loop control system design was illustrated. The closed-loop system response showed that the speed control goal was successfully achieved. The proposed modeling and control succeeded to reduce the speed overshoot and to increase the rise time while eliminating the steady-state speed error.

## REFERENCES

[1] S. Soylu, Electrical Vehicles – Modelling and Simulations, InTech Publication, 2011.
[2] J. Larminie, Electric Vehicle Technology, Willey Publication, 2013.
[3] Aalok Bhat, "Planning and Application of Electric Vehicle with MATLAB®/Simulink®," IEEE Trans. Veh. Technol., vol. 48, no. 6, Nov. 2016.
[4] www.mahindrae2o.com, Mahindra e2o Future of Mobility Brochure, 2013.

**5th IUGRC International Undergraduate Research Conference, Military Technical College, Cairo, Egypt, Aug 9th – Aug 12st, 2021.**